京都大学防災研究所年報 第48号B 平成17年4月
Annuals of Disas. Prev. Res. Inst., Kyoto Univ., No. 48 B, 2005

Development of a Scale Invariant Muskingum-Cunge Routing Method

Nawa Raj PRADHAN*, Yasuto TACHIKAWA and Kaoru TAKARA

*Graduate School of Civil Engineering, Kyoto University

Synopsis

It is found that a basin hydrological simulation in relations with drainage basin dominating geomorphological parameters is directly influenced by the scale of DEM resolution. A Scale Invariant model for the topographic index distribution (Pradhan *et al.*, 2004a) has fulfilled a part of this gap. A scale independent relationship in flood routing models in a distributed hydrological model is yet to be developed. To overcome this problem, scale laws that govern the relation in digital elevation data resolution on upslope contributing area has been analyzed and a mathematical formulation has been derived that successfully downscaled the upslope contributing area from coarse resolution DEM to target fine resolution DEM. The method to downscale the upslope contributing area is used to obtain the similar distribution of depth, cross-section and wave celerity from different DEM resolutions in Kamishiiba catchment (210 km^2) and to develop a scale invariant Muskingum-Cunge routing method.

Keywords: scale invariant, hydrological geomorphology, contributing area, Muskingum-Cunge routing

1. Introduction

Hydrological geomorphology is literally the interface between hydrology, the science of water and geomorphology, the study of landforms and their causative processes. Despite the enormous capacity of today's (and tomorrow's) information technologies, the complexity of the Earth's surface is such that the most voluminous descriptions are still only coarse generalizations of what is actually present. The need for continued and sustained research on scale issues in hydrological geomorphology is therefore self-evident.

Much of the spatial variability can be ignored at "small" spatial scales on the order of 0.1- 1.0m. Indeed, the scientific understanding of individual hydrologic processes at laboratory scales, such as flow through saturated and unsaturated columns of

porous media, is fairly well advanced. In particular, one wants to know how the laboratory-scale equations can be spatially integrated so as to describe the hydrologic cycle over a hillside. As the spatial scale under consideration increases to that of a single hillside, spatial variability becomes important, and new elements begin to influence the hydrologic mass balance, such as the topography of the hillside. With the development of the scale invariant model for the topographic index distribution, Pradhan *et al.* (2004) showed a possibility of spatially integrating the laboratory-scale equations to provide a consistent hydrologic mass balance in a topography driven model, TOPMODEL.

Beyond a single hillside, a river basin can be viewed as a channel-network-hills system. The hydrologic cycle for larger sub-basins involves the spatially integrated behaviors of several hills along a channel network. An understanding of the spatial variability among hillsides and their interactions through a channel network is necessary for this integration. Thus, at this point scale invariance in surface wave models finds an important component of the hydrologic cycle in river-basin hydrology. Although the relative importance of the components in the rainfall-runoff transformation process depends both on its working scale and on the geographical, climatic and environmental conditions of the site under consideration, the relative importance of routing phenomenon in surface flow hydrology cannot be ignored for a complete process model that offers a detailed description of the rainfall-runoff transformation.

The basic guide line set by this research to obtain physically based hydrological relationships independent of regions and scales is to develop an effective translation method of the scale dependence relations of the dominating hydrological and geomorphologic processes linked to typical properties of the catchment into effective hydrological model. Thus, this research is focused on the development of the scale invariance in catchment hydrology to develop a model consistent with observations. The model can be a potential tool to predict ungauged basins in an effective way.

Flow routing in channels has been a subject of much discussion for over half a century and more especially since the advent of digital computers. Flow routing is a technique for determining the propagation of flow from one point in the channel to another. Flow routing in open channels entails wave dispersion, wave attenuation or amplification and wave retardation or acceleration. These wave characteristics constitute the hydraulics of flow routing or propagation and are greatly affected by the geometric characteristics of channels. The flow variables whose propagation characteristics are of interest are discharge, velocity, depth, cross-section, volume and duration. Upslope contributing area is a key variable because of its intrinsic capability to describe the nested aggregation structure embedded in the fluvial landforms and its important physical implications (e.g., Rodriguez-Iturbe and Rinaldo, 1997; Leopold and Maddock, 1953). In catchment hill slope channel routing these flow variables is a function of upslope contributing area. In this research the scale dependence of the upslope contributing area is analyzed and a mathematical derivation to downscale the upslope contributing area has been proposed.

2. Development of Scale Invariant Model for the Upslope Contributing Area

In a DEM based distributed hydrological model, upslope catchment area at a point is the number of pixels draining through that point (Rodriguez-Iturbe and Rinaldo, 1997). In Figure 1(a), the smaller contributing area less than a km^2 that appears over

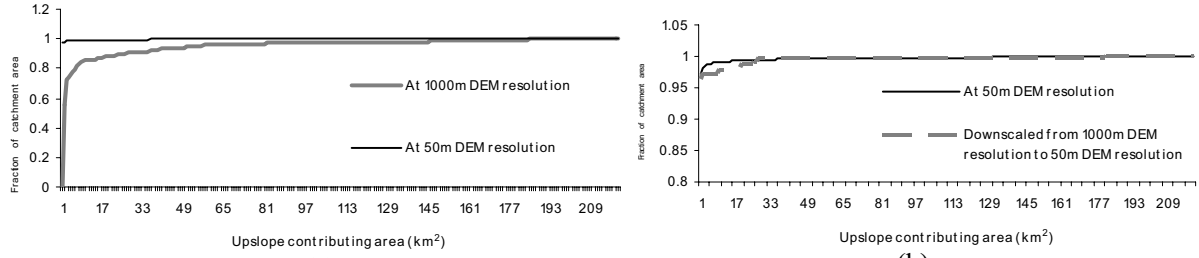

(a) (b)

Fig. 1 Comparison of upslope contributing area distribution function from different DEM resolutions in Kamishiiba catchment (210 km^2) (a) without downscaling method for upslope contributing area (b) with downscaling method for upslope contributing area.

97% in 50m DEM resolution is seen completely lost when 1000m DEM resolution is used.

The density of the small contributing area is higher in a catchment. In Figure 1(a), it is observed that this small contributing area less than a grid area of the coarse resolution DEM used is completely lost.

In fact the smallest contributing area derived from a DEM resolution is a single grid of the DEM at that resolution. Thus area smaller than this grid resolution is completely lost as the larger sampling dimensions of the grids act as filter. But as we use finer resolution DEM, the smaller contributing area - that is the area of finer grid resolution is achieved. From this point of view, we introduced number of sub grids N_s (see Figure 2) to derive scaled upslope contributing area as shown by Equation 1.

$$C_{i\,scaled} = \left(\frac{C_i}{N_s I_f} \right) \qquad (1)$$

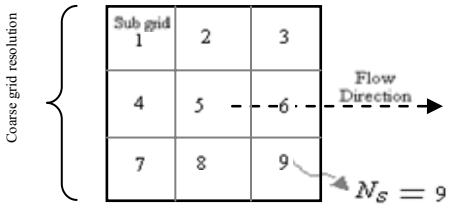

Fig. 2 Concept of N_s as sub grids within coarse grid resolution.

where the suffix i is a location in a catchment. $C_{iscaled}$ is the scaled upslope contributing area at a point i, I_f is a influence factor. N_s is the total number of subgrids within a coarse resolution grid. Figure 3 is an illustration to clarify the concept of N_s. Figure 3 shows 9 subgrids within a coarse resolution grid. The area of the coarse resolution grid shown in Figure 3 itself is the smallest contributing area for that DEM resolution. When this area of coarse resolution DEM is divided by the number of sub grids (i.e. 9 in Figure 3), that together adds up to make the coarse resolution grid, area of a sub grid as smallest contributing area for the target DEM resolution is obtained.

Figure 1(a) shows that in a catchment as the upslope contributing area gets bigger and bigger, the distribution of the contributing area values given by coarse and fine resolution DEM at the points downstream becomes closer and closer; thus the influence of N_s on C_i must gradually decrease in Equation (1). For this reason we introduced influence factor I_f in Equation (1) and I_f is described as;

$$I_f = e^{\left\{ \frac{(1-N_i)H}{N_o} \right\}} \qquad (2)$$

where, N_i is the number of the coarse resolution grids contained in the contributing area at a location i in the catchment, N_0 is the number of the coarse resolution

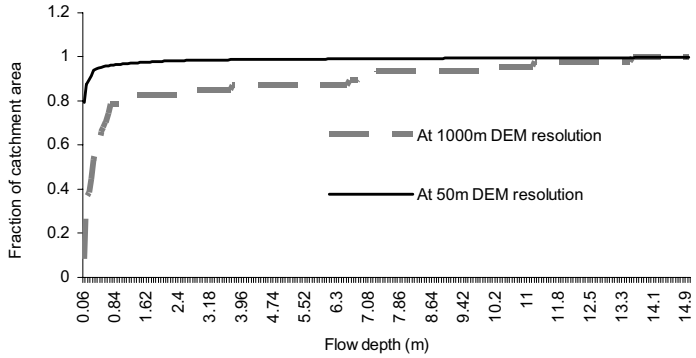

Fig. 3 Comparison of flow depth distribution from different DEM resolutions in Kamishiiba catchment (210 km^2).

grids contained in the contributing area at the outlet of the catchment. H in Equation (2) is introduced as harmony factor. Considering the influence of N_s on C_i in Equation (1) is almost negligible at the outlet of the catchment, the value of H can be obtained from Equation (3) as;

$$N_s e^{-H} = 1 \tag{3}$$

Finally, we developed a method to downscale the upslope contributing area from Equations (1) and (2) as;

$$C_{i\,scaled} = \left(\frac{C_i}{N_s e^{\left\{ \frac{(1-N_i)H}{N_o} \right\}}} \right) \tag{4}$$

Using Equation (4), the upslope contributing area is downscaled from 1000m DEM resolution to 50m DEM resolution. In contrast to Figure 1(a), Figure 1(b) shows the similar distribution of upslope contributing area from 50m DEM resolution and downscaled from 1000m DEM resolution to 50m DEM resolution.

3. Development of Scale Invariance in Surface Flow Hydrology

3.1 Development of method to downscale flow variables

A wave is a variation in flow, such as a change in flow rate or water surface elevation, and the wave celerity is the velocity with which this variation travels along the channel. The kinematic wave celerity, c_k, can be defined in terms of flow depth by Equation (5).

$$c_k = \frac{5}{3}\left(\frac{S_i^{1/2}}{n} \right) y_i^{2/3} \tag{5}$$

where S_i is the slope and n is the Manning's roughness coefficient. y_i is the depth of flow and is expressed as;

$$y_i = \left(\frac{nQ_i}{S_i^{1/2} B_i} \right)^{3/5} \tag{6}$$

where Q_i and B_i are the flow rate and channel width respectively at a point *i.*

In a distributed system routing the flow is calculated as a function of space and time through the system. The Manning's roughness coefficient n in

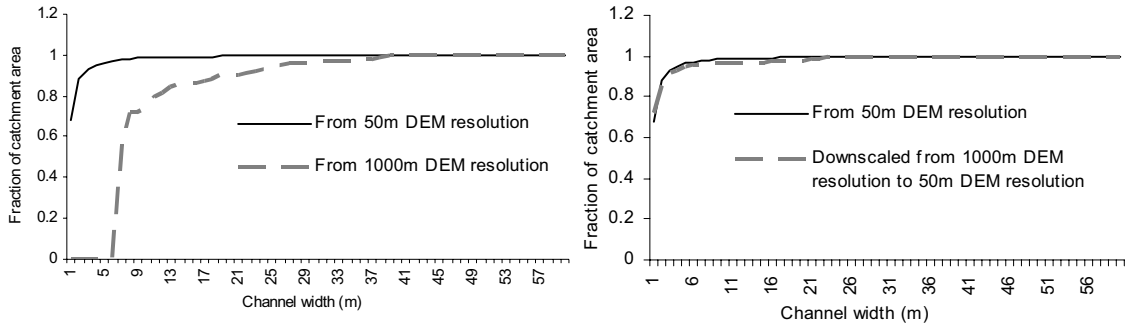

(a) (b)

Fig. 4 Comparison of channel width distribution from different DEM resolutions in Kamishiiba catchment (210 km^2) (a) without downscaling method introduced (b) with downscaling method introduced.

Equation (5) and (6) is an effective parameter. Figure 3 shows much difference in distribution of depth y_i from 50m DEM resolution and from 1000m DEM resolution when keeping the same value of Manning's roughness coefficient for the 1000m DEM resolution, identified at 50m DEM resolution (0.025 in Table 1). This scale problem in depth has serious impact on the hydrologic response of a distributed routing method (wave characteristics).

The root of this problem originates from the scale problem on upslope contributing area as discussed earlier in section 2.1 and in figure 1(a), and also from the underestimation of slope in coarse resolution DEM. Upslope contributing area is a key variable because of its intrinsic capability to describe the nested aggregation structure embedded in the fluvial landforms and its important physical implications (e.g., Rodriguez-Iturbe and Rinaldo, 1997).

(1) Deriving channel width information at finer scale

In hill slope channel routing, one of the difficult task is defining the channel width. The channel width less than the DEM grid resolution used cannot be obtained. Although the channel width is obtained as a function of upslope contributing area or discharge as explained by Leopold and Maddock (1953), the width of reaches still cannot be obtained where the finer information of upslope contributing area or discharge taken as independent variable is filtered out. Here, channel width is derived as a function of upslope contributing area as given by Equation (7).

$$B_i = aC_i^b \tag{7}$$

where B_i is the channel width at a location i and C_i is the upslope contributing area at that location. a and b are the coefficients. The coefficients a and b are assigned as 7.0 and 0.4 respectively. In Figure 4 (a) it is shown that the percentage of smaller width values is much lesser when using 1000m DEM resolution then when using 50m DEM resolution. Thus scaled upslope contributing area from Equation (4) is introduced in Equation (7). The downscaled channel width at a location i, $B_{iscaled}$ is given as;

$$B_{i\ scaled} = aC_{iscaled}^{\ b} \tag{8}$$

Table 1. Effective parameter values identified at 50m DEM resolution in Kamishiiba catchment (210 km^2).

Lateral transmissivity of soil at saturation condition, *To* [m^2/hr]	Manning's roughness coefficient *n*
9.8	0.025

In Figure 4 (b) it is shown that the distribution of downscaled channel width from 1000 m DEM resolution to 50m DEM resolution and that from 50m DEM resolution has matched. Thus, by using Equation (8) we successfully obtained the loss portion of channel width at finer scale, 50m DEM resolution, by using only coarse resolution DEM, 1000m DEM resolution.

(2) Deriving discharge information at finer scale

As the drainage area increases downstream, the actual discharges in downstream reaches also increases. Flow rate Q_i is a function of upslope contributing area (Strahler, 1964).

Discharge values produced by areas smaller than a grid size in the DEM is completely lost as the larger sampling dimensions of the grids act as filter. But as we use finer resolution DEM, the smaller discharge values - that is the discharge values produced by finer grid resolution is achieved. Thus as in Equation 4 we introduced number of sub grids, N_s, and influence factor I_f as the downscaling factors for discharge as shown in Equation (9).

$$Q_{i\,target} = \left(\frac{Q_i}{N_s e^{\left\{ \frac{(1 - N_i)H}{N_o} \right\}}} \right) \qquad (9)$$

(3) Deriving flow depth information at finer scale

Substituting Q_i ,B_i and S_i in Equation (6) by $B_{iscaled}$ and $Q_{itarget}$ from Equations (8) and (9), and by θ_{scaled} (refer Pradhan *et al*., 2004 for details of the derivation of θ_{scaled}) respectively we develop the method to downscale the flow depth, $y_{iscaled}$ as;

$$y_{iscaled} = \left(\frac{nQ_{it\,target}}{\theta_{scaled}^{1/2} B_{iscaled}} \right)^{3/5} \qquad (10)$$

In Figure 5 (all the simulation results in Figure 5 are made at time step 43 hours of the rainfall event), it is shown that the distribution of downscaled flow depth from 1000 m DEM resolution to 50m DEM resolution and that from 50m DEM resolution (Manning's roughness coefficient *n* used is identified at 50m DEM resolution, refer Table 1) has matched. Thus, by using Equation (10) we successfully reduced the over estimation of depth given by 1000m DEM resolution (shown in Figure 5).

Several variations of the kinematic wave routing method have been proposed. These routing methods can be easily coupled with the proposed downscaling methods of the dominating geomorphometric parameters and flow variables to develop a scale invariant routing method.

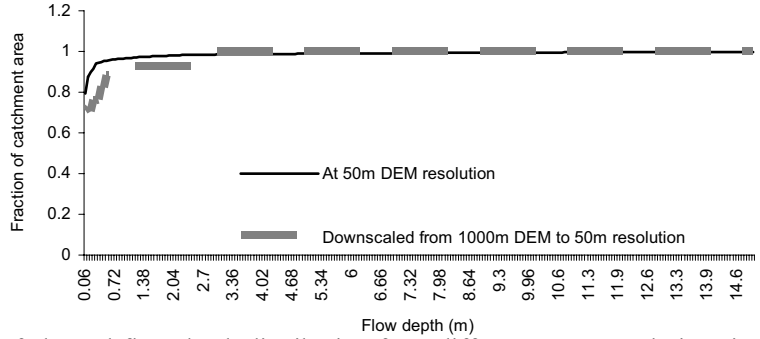

Fig. 5 Comparison of channel flow depth distribution from different DEM resolutions in Kamishiiba catchment (210 km^2) with applying the downscaling method.

3.2 Development of Scale Invariant Muskingum-Cunge Routing Method

Cunge (1969) proposed that Muskingum method can be considered an approximate solution of a modified diffusion equation. The diffusion, implying the decay of the flood-wave concentration (discharge or stage) during flood-wave propagation downstream, can be attributed to the magnitude of the pressure gradient and inertia terms (Ponce, 1982). In most practical cases, the inertia term is much smaller than the pressure-gradient term. The various forms of the diffusion wave approximation of the St. Venant equations for flood-wave propagation in open channels are presented (Keefer and McQuivey, 1974; Gonwa and Kavvas, 1986). Cunge (1969) established the link between the Muskingum method and convection-diffusion equation. He advanced the interpretation of the Muskingum method as a finite-difference analog of the kinematic wave equation, and the numerical diffusion emanating from its application was linked to the physical diffusion of the convection-diffusion equation. In flood routing, a normal rating is implicitly assumed at the downstream boundary. This assumption may not hold in many practical cases, in which cases the downstream boundary condition needs to be specified, that complicates the routing problem. Specification of the down-stream routing condition is complicated by the existence of a hysteresis loop in the rating curve due to unsteady nature of the flow. Ponce (1991) argues that these limitations may be overcome by such practical alternatives as the Muskingum-Cunge method by tying the numerical diffusion of the Muskingum method to the physical diffusion of the diffusion wave model. This permits the solution of the diffusion wave equation by solving the Muskingum method, subject to the matching of numerical and physical diffusivities. This technique may provide the link between hydrologic and hydraulic methods of flood routing. Although there are advantages in adopting the Muskingum-Cunge routing method to simulate the surface runoff, the method is seriously influenced by the DEM resolution used.

The kinematic wave equation is derived from the continuity equation as;

$$\frac{\partial A}{\partial t}+\frac{\partial Q}{\partial x}=0 \qquad (11)$$

and can be expressed in discharge, Q, as the dependent variable for a channel as;

$$\frac{1}{c}\frac{\partial Q}{\partial t}+\frac{\partial Q}{\partial x}=0, \qquad 0<x<L \qquad (12)$$

where A is the area of flow cross section, c the travel speed of the flood wave, called the kinematic wave speed (celerity).

Cunge (1969) proposed an explicit finite-difference scheme for solution of Equation (12), which may also serve as a basis for a generalized treatment of kinematic wave models. The scheme centers the time derivative by taking weighting factor in time direction=0.5 and retains the weighting coefficient x in space. The celerity c is taken to be an average constant value for the reach or computational cell as;

$$\frac{1}{c}=\left(\frac{dA}{dQ}\right)_x=\frac{1}{\Delta x}\int_{\Delta x}\left(\frac{dA}{dQ}\right)_x dx=\left\langle\left(\frac{dA}{dQ}\right)_x\right\rangle=\left\langle\frac{1}{c}\right\rangle\approx\frac{1}{\langle c\rangle} \qquad (13)$$

where $\langle . \rangle$ signifies the average.

Equation (12) can be written in finite-difference form as;

$$\frac{1}{c\Delta t}\left[(1-x)\left(Q_{i+1}^{j+1}-Q_{i+1}^{j}\right)+x\left(Q_i^{j+1}-Q_i^{j}\right)\right]+\frac{1}{2\Delta x}\left[Q_{i+1}^{j}-Q_i^{j}+Q_{i+1}^{j+1}-Q_i^{j+1}\right]=0 \qquad (14)$$

By solving for Q_{i+1}, Equation (14) can be written as

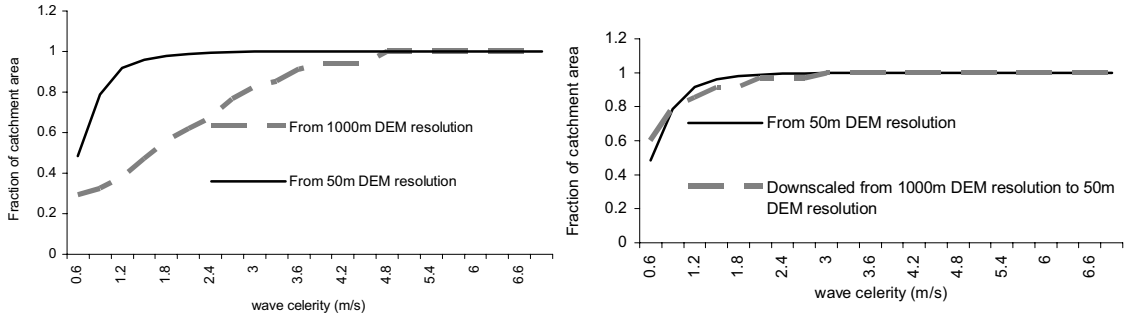

(a) (b)

Fig. 6 Comparison of wave celerity distribution from different DEM resolutions in Kamishiiba catchment (210 km^2) (a) without downscaling method for kinematic wave celerity (b) with downscaling method for kinematic wave celerity.

the classical Muskingum equation, as;

$$Q_{i+1}^{j+1} = C_1 Q_i^j + C_2 Q_i^{j+1} + C_3 Q_{i+1}^j \tag{15}$$

or, $$Q_4 = C_1 Q_1 + C_2 Q_2 + C_3 Q_3$$

where
$$C_1 = \frac{\Delta t + 2xK}{2K(1-x) + \Delta t} \tag{16a}$$

$$C_2 = \frac{\Delta t - 2xK}{2K(1-x) + \Delta t} \tag{16b}$$

$$C_3 = \frac{2K(1-x) - \Delta t}{2K(1-x) + \Delta t} \tag{16c}$$

and
$$K = \frac{\Delta x}{c} \tag{17}$$

where K is the flood travel time over a reach with length Δx

$C_1+C_2+C_3=1$

The unit of K is time, and it has the connotation of storage delay time, travel time, translation time, or lag time.

Cunge (1969) has shown that equations (15) to (17) constitute a second-order approximation of the diffusion wave equation if the weighting coefficient x is evaluated as

$$x = \frac{1}{2}\left(1 - \frac{Q}{B\theta\, c\Delta x}\right), \quad 0 < x < 0.5 \tag{18}$$

where θ is the channel bed slope. Cunge derived Equation (18) from a Taylor series expansion of $Q(x_i, t_j)$ in the finite-difference form of Equation (12) and a comparison with the coefficients of the diffusion wave equation for regular channels. The value of x is found to depend on Δx (V. P. Singh, 1996).

Earlier we analyzed the scale dependence and developed the downscaling methods of the dominating geomorphometric parameters and flow variable whose propagation characteristics are of interest in surface flow hydrology. K and x in Equation (17) and Equation (18) governs the influence of routing in surface flow hydrologic response in Muskingum-Cunge routing method. The flood wave travel time is derived from wave celerity. The weighting coefficient x in Equation (18) is also dependent on wave celerity. Thus wave celerity is a governing factor in Muskingum-Cunge routing method. The propagation speed or celerity of a flood wave is one of the main properties of the flood-wave propagation and is related directly to the wave deformation and attenuation. Hence an investigation into scale effect in celerity is essential for deriving the scale invariance of flood-wave propagation.

In Figure 6 (a) (all the simulation results in Figures 6 (a) are made at time step 43 hours of the

rainfall event), it is shown that the distribution of celerity from 1000 m DEM resolution is much biased as compared with that from 50m DEM resolution (Manning's roughness coefficient n used is identified at 50m DEM resolution).

Substituting y_i and S_i in Equation (5) by $y_{iscaled}$ and θ_{scaled} we developed the method to downscale the wave celerity distribution as.

$$c_{kiscaled} = \frac{5}{3}\left(\frac{\theta_{iscaled}^{1/2}}{n}\right) y_{iscaled}^{2/3} \qquad (19)$$

In Figure 6 (b) (all the simulation results in Figures 6 (b) are made at time step 43 hours of the rainfall event), it is shown that the distribution of downscaled celerity from 1000 m DEM resolution to 50m DEM resolution, by using Equation (19), and that from 50m DEM resolution (Manning's roughness coefficient n used is identified at 50m DEM resolution) has matched. Thus, by using Equation (19) we successfully reduced the over estimation of celerity given by 1000m DEM resolution.

Substituting c of Equation (17) by $c_{iscaled}$ from Equation (19) the downscaling method of K is defined as:

$$K_{iscaled} = \frac{\Delta x}{c_{iscaled}} \qquad (20)$$

Substituting c in Equation (18) by $c_{iscaled}$ from Equation (19); B in Equation (18) by $B_{iscaled}$ from Equation (8) and θ by $\theta_{iscaled}$ (derivation of $\theta_{iscaled}$ is presented in Discussion) the downscaling method of x is defined as:

$$x_{iscaled} = \frac{1}{2}\left(1 - \frac{Q_{iscaled}}{B_{iscaled}\theta_{iscaled}\, c_{iscaled}\Delta x}\right) \qquad (21)$$

Equations (20) and (21) are introduced in Muskingum-Cunge routing method to develop Scale Invariant Muskingum-Cunge routing method.

4. RESULTS AND DISCUSSION

It is particularly surface water hydrology that interacts with geomorphology although recently there has been an increasing convergence between research in geomorphology and in groundwater hydrology. One of the main reasons of this increasing convergence between research in geomorphology and in groundwater hydrology is to define processes of runoff production and to solve the problem of what to route before deciding how to route (Cordova and Rodriguéz-Iturbe, 1983). If this argument is accepted then scale issues in runoff production mechanism should be solved prior to finding a scale invariance in surface flow routing mechanism.

In addition to relations between drainage basin characteristics and basin hydrological response, geomorphologists have made particular contributions in the investigation of runoff producing areas and the dynamic ways in which such areas contribute to the generation of stream hydrographs, including headwater drainage systems and the modeling of their role in runoff production, TOPMODEL (Beven and Kirkby, 1979). We use TOPMODEL, saturation excess runoff production mechanism, to generate overland water quantity for routing.

Figure 7 shows how the DEM resolution effects on the runoff producing areas. Figure 7 (a) shows 7% saturated area at 50m DEM resolution. On the other hand when using 1000m DEM resolution and parameters identified at 50m DEM resolution, the saturated area increased to 59%, in Figure 7 (b), which is physically unacceptable identification of a conceptual state variable. This results primarily from the DEM resolution effect on topographic index distribution (Zhang and Montgomery, 1994).

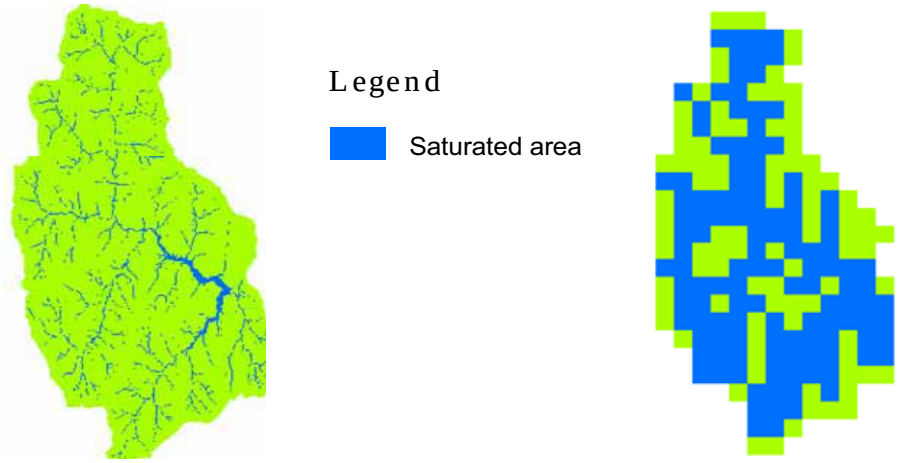

(a) (b)

Fig. 7 Comparison of saturated area in Kamishiiba catchment (210 km^2), at initial state, at different DEM resolutions. (a) Saturated area 7% at 50m DEM resolution (b) Saturated area 59% at 1000m DEM resolution. In both the case same parameters identified by 50m DEM resolution TOPMODEL is used.

To solve this problem we coupled TOPMODEL with the Scale Invariant model for topographic index distribution (Pradhan et. al. 2004) as defined by Equation (22):

$$TI_{scaled} = \ln\left(\frac{C_i}{W_i R_f \theta_{scaled}}\right) \qquad (22)$$

where TI_{scaled} is the scaled topographic index, C_i is the upslope contributing area of the coarse resolution DEM and W_i is the unit contour length of coarse resolution DEM, i is a location in catchment. R_f is a resolution factor defined by Equation (23):

$$R_f = \frac{Coarse\ \ DEM\ \ \text{Re}solution}{T\text{arg}et\ \ DEM\ \ \text{Re}solution} \qquad (23)$$

R_f in Equation (23) is introduced to obtain from the coarse resolution DEM, the lost of higher density of the lower value of upslope contributing area per unit contour length found in finer, target, resolution DEM. Details of Equation (23) derivation is given in Pradhan *et al.* (2004). θ_{scaled} in Equation (22) is the downscaled steepest slope of the target resolution DEM (refer Pradhan *et al.*, 2004a for details of the derivation of θ_{scaled}).

Figure 8 (b) shows that with scaled topographic index distribution from 1000m to 50m DEM resolution, the saturated area obtained dropped down very close to that obtained at 50m DEM resolution, in Figure 8 (a). This is how the physical basis of the model is retained with the scale invariant model.

Figure 9 (a) is the 50m DEM resolution TOPMODEL simulation. Obviously the simulated hydrograph from TOPMODEL alone is bias with observed one with sharp increase in peaks, indicating quick response to the rainfall and no time delay in the surface flow hydrologic response (without taking into account of location of the overland water generated from the outlet and the time delay). Thus the peak flows (that signifies the contribution of surface runoff) are seen ahead of the actual hydrologic response of the catchment, the observed flow. This shows the importance of the routing delays in forming the hydrograph. Figure 9 (b) shows the simulation result with Muskingum-Cunge routing method that has smoothened the simulated hydrograph with 95% Nash efficiency.

Figure 10 shows the simulation results from 1000m DEM resolution. A huge bias in predicted

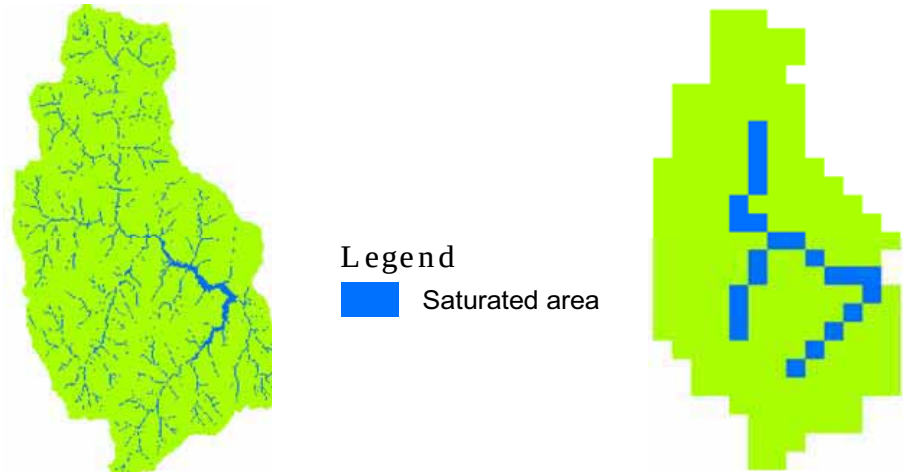

(a) (b)

Fig. 8 Comparison of saturated area in Kamishiiba catchment (210 km^2), at initial state, at different DEM resolutions. (a) Saturated area 7% at 50m DEM resolution (b) Saturated area 10% when downscaling the topographic index distribution from 1000m DEM to 50m DEM resolution. . In both the case same parameters identified by 50m DEM resolution TOPMODEL is used.

simulated discharge, as a consequence of overestimation of saturated area in Figure 7 (b), is seen when the same 50m DEM resolution TOPMODEL parameters, *To* value in Table 1, are used at 1000m DEM resolution too. In Figure 10, it is also shown that the similar simulated discharge condition as shown in Figure 9 (a) is obtained from the 1000m DEM resolution too by downscaling the topographic index distribution. Thus scale independent runoff production mechanism is successfully obtained.

After obtaining the scale independent runoff production mechanism, the simulation result also shown in Figure 11 (a), we applied the Muskingum-Cunge routing method with the same effective value of the Manning's roughness coefficient *n* identified at 50m DEM resolution Muskingum-Cunge routing method. Figure 11 (b) shows the routing effect in this case. Obviously, the routing effect at 1000m DEM resolution shown by Figure 11 (b) is not as effective as that at 50m DEM resolution, shown by Figure 9 (b), when applying the same effective parametric value of *n*. Figure 11 (b) clearly lacks the required attenuation effect and the hydrograph response is still seen quicker than the actual catchment discharge response.

In scale issues, this lack in the appropriate attenuation and routing delays in the simulated

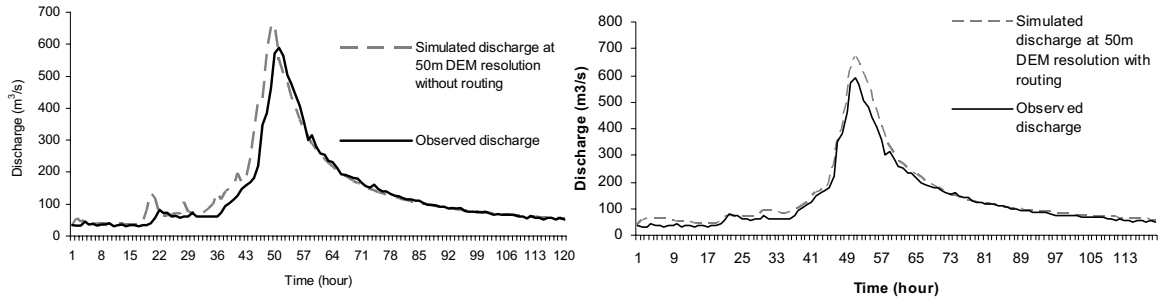

(a) (b)

Fig. 9 Comparison of observed and the simulated hydrograph at 50m DEM resolution in Kamishiiba catchment (210 km^2). (a) without routing (b) with Muskingum-Cunge routing method.

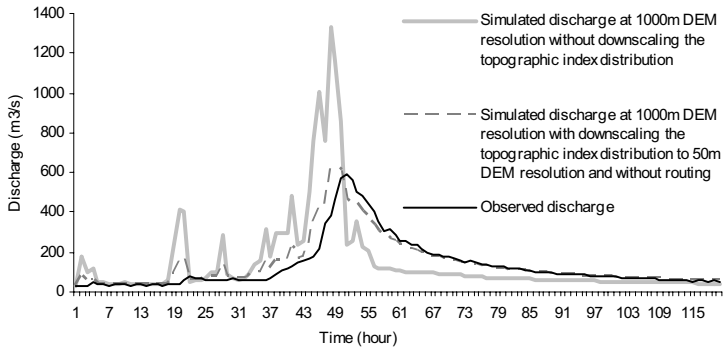

Fig. 10 Comparison of simulation result in Kamishiiba catchment (210 km^2) from scale independent runoff production mechanism. In all the simulation results, 50m DEM resolution TOPMODEL identified parameters are used.

hydrograph originates from reduced travel distance of the flood wave when the coarse resolution DEM is used as compared to the travel distance of the flood wave in the finer resolution DEM. Earlier we discussed the scale effect in the runoff generation mechanism. Scale independent runoff generation mechanism is shown by Figure 8 (b). Analyzing Figure 8 (a) and 8 (b), it is found that the saturated area is almost equal but the travel distance for the water generated in Figure 8 (b) is much shorter than for the water generated in Figure 8 (a) before reaching the outlet. This makes us clear that even after obtaining the scale invariance in runoff generation mechanism, the saturated area in coarser DEM resolution is more concentrated closer to the outlet whereas in finer resolution DEM, the saturated area extends further upslope. Thus the lag time of the hydrograph response in Figure 8 (b) is much shorter then in Figure 8 (a). This is why the same effective parametric value of n that fit the simulated hydrograph at 50m DEM resolution in Figure 9 (b) could not produce an appropriate delay in translation time as shown in Figure 10 (b).

At this point an obvious question that can be raised is what if the whole catchment is actually contributing the runoff. If this is the case then every point in a catchment is producing the runoff either by saturation excess overland flow mechanism or infiltration excess overland flow mechanism. In this case too, we analyzed that the response time of the flood wave in routing is much delayed when using fine resolution DEM instead of coarse resolution

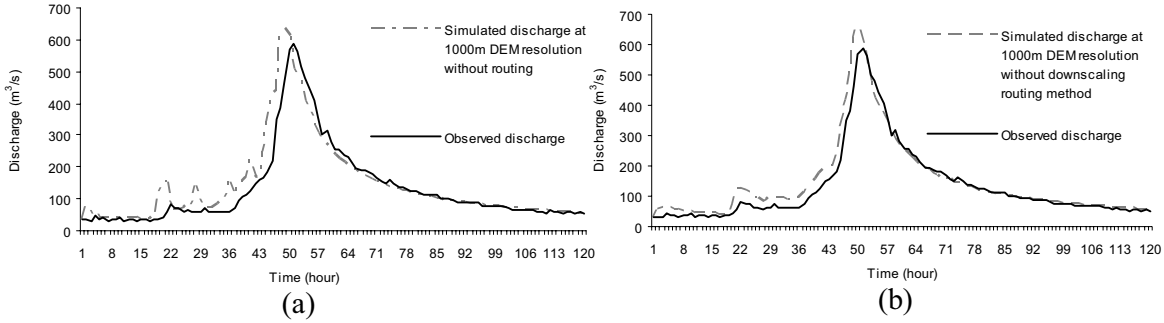

Fig. 11 Analysis of Muskingum-Cunge routing effect in Kamishiiba catchment (210 km^2) at 1000m DEM. (a) simulation result at 1000m DEM resolution from scale independent runoff production mechanism (b) Adding Muskingum-Cunge routing with Manning's roughness coefficient identified at 50m DEM resolution in the simulation result of Figure 9 (b).

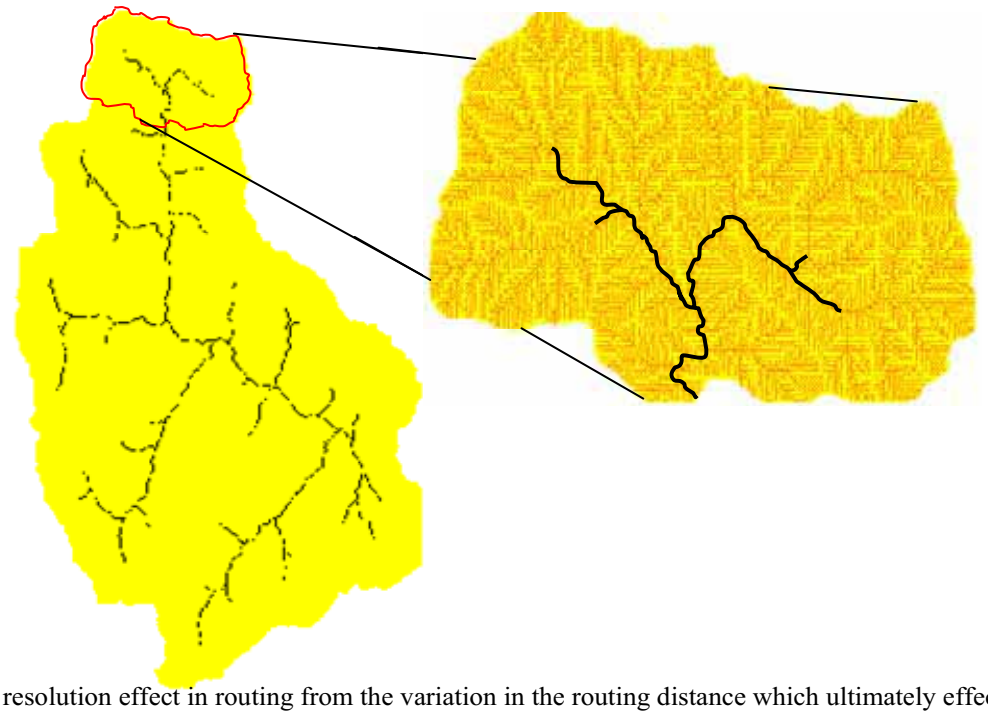

Fig. 12 DEM resolution effect in routing from the variation in the routing distance which ultimately effects in travel time and time of concentration of the flood wave.

DEM. This is clearer from Figure 12. The bold black lines in Figure 12 shows the points equal or more than 1 km^2. Enlarging the small subcatchment we can see the fine drainage network that is obtained from 50m DEM resolution. Thus before accumulating the surface runoff at the points where the contributing area is equal or more than 1 km^2 as shown by the bold black line, the surface runoff has to be routed through out this finer drainage network. This produces the routing delay. But on the other hand, this portion of the routing delay if we take 1000m DEM resolution, does not take part as the water is instantly accumulated in a 1 km^2 of a grid. Thus using 1000m DEM resolution the routed hydrograph response is faster as the routed distance is shorter. If the DEM is infinitely small the routing length is infinitely large and hence the time of concentration. In this research we do not come up with a threshold measurement scale.

From the above discussion it is clear that the DEM resolution effect in routing arises from the variation in the routing distance which ultimately effects in travel time and time of concentration of the flood wave. In Muskingum-Cunge routing method K parameter defined by Equation (17) is the flood travel time over a reach with length Δx, and it has the connotation of storage delay time, travel time, translation time, or lag time (Singh, 1996). We propose a method to downscale this K parameter as defined by Equation (20). Thus the underestimation of this travel time is increased by the downscaling method as shown by Figure (13).

After obtaining the scale independent runoff routing mechanism and Scale Invariant Muskingum-Cunge routing method that we propose in this paper, we applied it to the simulation process with the same effective value of the Manning's roughness coefficient n identified at 50m DEM resolution Muskingum-Cunge routing method. Figure 14 (b) shows that the appropriate attenuation and routing delays has been formed in the simulated hydrograph. The Nash efficiency increased from 92%

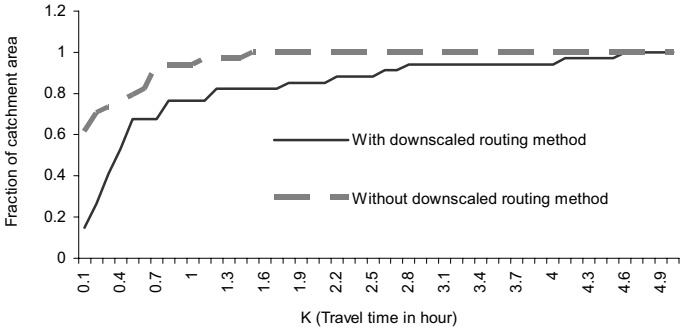

Fig. 13 Increament of the travel time defined by the Muskingum-Cunge parameter K when the downscaling method is applied.

in Figure 14 (a) to 94% in Figure 14 (b). Thus, the similar simulated hydrograph calibrated at 50 m DEM resolution, in Figure 9 (b), is also obtained from 1000m DEM resolution, in Figure 14 (b). Thus the compulsion to increase the effective parametric value of *n* when using coarser resolution DEM so that could compensate the underestimation of travel time as discussed in Figures 8 and 12 is eliminated with the downscaling method of routing proposed in this paper. This has made possible to link *n* parameter across scales in a distributed routing method.

5. Conclusion

There is a long tradition in geomorphology of seeking generalizable rules for landscape evolution such that real landscapes, and particularly their scale-dependent attributes, can be modeled. However, basin hydrological response in relations with the geomorphological parameters are influenced by DEM resolution. In this research we analyzed the scale laws that govern the relation in digital elevation data resolution on upslope contributing area and developed a mathematical formulation to downscale the upslope contributing area. The method to downscale the contributing area is successfully applied to downscale the flow variables to develope a scale invariant model in surface flow hydrology. We coupled these downscaling methods of the flow variables, whose propagation characteristics are of interest, in the Muskingum-Cunge routing method and developed a Scale Invariant Muskingum-Cunge

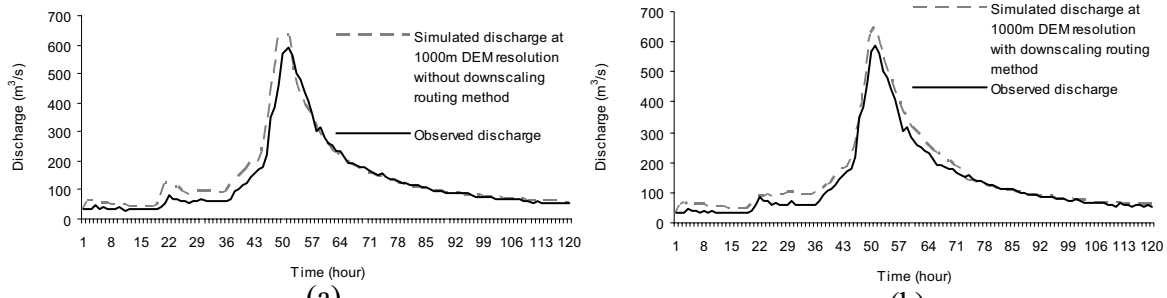

Fig. 14 Analysis of Muskingum-Cunge routing effect in Kamishiiba catchment (210 km^2) at 1000m DEM. (a) simulation result at 1000m DEM resolution without downscaling the Muskingum-Cunge routing method (b) simulation result at 1000m DEM resolution with downscaling the Muskingum-Cunge routing method. In both the case, the effective parametric value of Manning's roughness coefficient, *n*, used is identified at 50m DEM resolution and with scale independent runoff production mechanism.

routing model. This has enhanced the consistency across the scales of the DEM resolution dependent parametric value like Manning's roughness coefficient *n*. It is hoped that the findings of this research seek its applicability as a tool to a wider range of boundary as per the scale problems in hydrological processes and solution approach is concerned.

References

Beven, K., J. and Kirkby, M., J. (1979): A physically based, variable contributing area model of basin hydrology, *Hydrological Science Bulletin,* Vol. **24,** pp**.** 43-69.

Cunge, J., A. (1969): On the subject of a flood propagation computation method (Muskingum Method), *Journel of Hydraulic Research* Vol. **7**, pp. 205-230.

Cordova, J., R. and Rodriguez-Iturbe, I. (1983): Geomorphoclimatic estimation of extreme flow probabilities, *Journal of Hydrology*, Vol. 65, pp. 159-173.

Gonwa, W., S. and Kavvas, M., L. (1986): A modified diffusion equation for flood propagation in trapezoidal channels, *Journal of Hydrology*, Vol. 83, pp. 119-136.

Keefer, T., N. and McQuivey, R., S. (1974): Multiple linearization flow routing model, *Journal of the Hydraulics Division*, *ASCE*, Vol. 100, No. HY7, pp. 1031-1046.

Leopold, L., B. and Maddock, T. (1953): The hydraulic geometry of stream channels and some physiographic implications, *U.S. Geol. Surv. Prof. Paper, 252.*

Ponce, V., M. (1982): Nature of wave attenuation in open channel flow, *Journal of the Hydraulics Division, ASCE*, Vol. 108, No. HY2, pp. 257-261.

Ponce, V., M. (1991): New perspective on the Vedernikov number, *Water Resources Research*, Vol. 27, pp. 1777-1779.

Pradhan, N., R., Tachikawa, Y. and Takara, K. (2004): A scale invariance model for spatial downscaling of topographic index in TOPMODEL, *Annual Journal of Hydraulic Engineering, JSCE,* Vol. **48,** pp. 109-114.

Rodriguez-Iturbe, I. and Rinaldo, A. (1997): *Fractal River Basins: Chance and Self-organization,* Cambridge University Press.

Singh, V., P. (1996): *Kinematic Wave Modeling in Water Resources: Surface-Water Hydrology,* Wiley Interscience, New York.

Strahler, A., N. (1964): Quantitative geomorphology of drainage basins and channel networks, *Handbook of Applied Hydrology*, Chow, V., T. (ed.), Section 4-2, McGraw-Hill, New York.

Zhang, W. and Montgomery, D., R. (1994): Digital elevation model grid size, landscape representation, and hydrologic simulations, *Water Resources Research,* Vol. 30, pp. 1019-1028.

スケールに依存しないマスキンガム－クンジ河道流追跡法の開発

ナワラジプラダン*・立川康人・寶　馨

*京都大学大学院工学研究科土木工学専攻

要　旨

流域の地形的特性に支配されるモデルパラメータを有する水文シミュレーションは，数値地形モデルの空間分解能に直接影響を受ける。このスケール依存性を解決するために，Pradhan ら(2004)は地形指標のダウンスケールを実現することによるスケール不変モデルを提案している。本研究では，この研究を発展させて，分布水文モデルにおける河道追跡モデルを対象とするスケール不変モデルを提案する。このために，対象地点上流の流域面積に対する数値地形データの空間分解能のスケール依存性を分析し，ダウンスケールのために数理モデルを提案する。このモデルでは，空間分解能の細かい数値地形モデルを用いて得た流域面積を，空間分解能の粗いデータを用いて得ることが可能である。この手法を，水深，通水断面積，伝播速度に適用し，上椎葉流域を対象として，マスキンガム－クンジ河道流追跡法を開発した。

キーワード：スケール不変，水文地形学, 流出寄与域，マスキンガム－クンジ河道追跡法